

Appearance of hepatocellular adenomas on gadoxetic acid-enhanced MRI

Timm Denecke · Ingo G. Steffen · Sheela Agarwal ·
Daniel Seehofer · Thomas Kröncke ·
Enrique Lopez Hänninen · Incken-Birthe Kramme ·
Peter Neuhaus · Sanjay Saini · Bernd Hamm ·
Christian Grieser

Received: 8 December 2011 / Revised: 12 January 2012 / Accepted: 21 January 2012 / Published online: 22 March 2012
© European Society of Radiology 2012

Abstract

Objective The purpose of this study was to evaluate enhancement characteristics of hepatocellular adenomas (HCAs) using gadoxetic acid as a hepatocyte-specific MR contrast agent.

Methods Twenty-four patients with histopathologically proven HCAs were retrospectively identified. MRI consisted of T1- and T2-weighted (w) sequences with and without fat saturation (fs), multiphase dynamic T1-w images, and fs T1-w images during the hepatobiliary phase. Standard of reference was surgical resection ($n=19$) or biopsy ($n=5$). Images were analysed for morphology and contrast behaviour including signal intensity (SI)

measurement on T1-w images normalised to the pre-contrast base line.

Results In total 34 HCAs were evaluated. All HCAs showed enhancement in the arterial phase; 38 % of HCAs showed reduced contrast enhancement (“wash-out”) in the venous phase. All HCAs showed enhancement (SI increase, 56 ± 53 %; $P < 0.001$) in the hepatobiliary phase, although liver uptake was stronger (96 ± 58 %). Thus, 31 of all HCAs (91 %) appeared hypointense to the surrounding liver in the hepatobiliary phase, while 3 out of 34 lesions were iso-/hyperintense.

Conclusions Gadoxetic acid accumulates in HCAs in the hepatobiliary phase, although significantly less than in surrounding liver. Thus, HCA appears in the vast majority of cases as a hypointense lesion on hepatobiliary phase images.

Key Points

- *Magnetic resonance-specific contrast agents are now available for hepatic imaging.*
- *Hepatocellular adenomas enhance with gadoxetic acid as in previous CT/MRI experience.*
- *Enhancement during the hepatobiliary phase is less in HCAs than in liver.*
- *Typical HCAs appear as hypointense lesions on T1-w hepatobiliary phase images.*
- *True hyperintense HCA enhancement can occasionally occur during the hepatobiliary phase.*

The data were presented at the ESGAR and RSNA in 2011.

T. Denecke · I. G. Steffen · T. Kröncke · E. L. Hänninen ·
B. Hamm · C. Grieser (✉)
Klinik für Radiologie, Campus Virchow-Klinikum,
Charité–Universitätsmedizin Berlin,
Augustenburger Platz 1,
13353 Berlin, Germany
e-mail: christian.grieser@charite.de

D. Seehofer · P. Neuhaus
Klinik für Allgemein, Viszeral- und Transplantationschirurgie,
Campus Virchow-Klinikum, Charité–Universitätsmedizin Berlin,
Berlin, Germany

I.-B. Kramme
Institut für Pathologie, Campus Virchow-Klinikum,
Charité–Universitätsmedizin Berlin,
Berlin, Germany

S. Agarwal · S. Saini
Department of Radiology, Harvard Medical School
and Massachusetts General Hospital,
Boston, MA, USA

Keywords MRI · Hepatocellular adenoma · Adenoma ·
Liver · Gadoxetic acid

Introduction

Hepatocellular adenomas (HCAs) are benign lesions that typically occur in healthy young and middle-aged women

with an estimated incidence of 3–4 per 100,000 per year in long-term oral contraceptive users [1–3]. HCAs can also be found in men using anabolic steroids, and in patients with glycogen storage disease or metabolic syndrome [4]. HCAs carry a risk of spontaneous bleeding and malignant transformation into hepatocellular carcinoma (HCC) and therefore surgical removal of large, haemorrhagic, or atypical-appearing HCAs should be considered [5, 6]. Therefore, identification of HCAs and differentiation from focal nodular hyperplasia (FNH) and malignant entities is a common problem in liver imaging.

Contrast-enhanced magnetic resonance imaging (MRI) is a highly accurate non-invasive imaging technique for the detection and characterisation of solid focal liver lesions including HCAs [7, 8]. During the past 6 years, a new T1-w based positive contrast agent, gadoxetic acid (Gd-EOB-DTPA, Primovist or Eovist; Bayer Schering Pharma, Berlin, Germany), which shows intracellular uptake in hepatocytes with a hepatic extraction fraction of approximately 50 %, has been approved for liver imaging in many countries worldwide [9–12]. The hepatocytic uptake of gadoxetic acid and thus hepatic MR enhancement are mediated by the organic anionic transport peptide (OATP) family; these peptides are located, for example, at the apical membrane of hepatocytes [13]. In humans, OATP1B1 and OATP1B3 are presumably the most important transporters for gadoxetic acid uptake into hepatocytes [14–16]. OATP transports a wide range of drugs (e.g. antibiotics); however, compared with the findings of an *in vivo* animal study, no metabolic interaction of gadoxetic acid and these drugs was found in healthy volunteers [13, 17, 18].

It has been shown that gadoxetic acid improves detection and characterisation of benign and malignant hepatic lesions by its specific properties [9, 11]. Furthermore, in case of a positive OATP1B1 and/or -1B3 expression, a significantly higher hepatocyte-selective enhancement of hepatic lesions such as HCC may be seen [19]. However, to date there are only few reports with a small number of cases on the imaging findings of HCAs with gadoxetic acid [10, 11, 20].

Therefore, the purpose of the present study was to determine the MRI findings and the contrast enhancement with gadoxetic acid in a larger patient group with histopathologically proven HCAs.

Materials and methods

Patients

In a bicentric study, all patients with HCAs who had undergone liver MRI with gadoxetic acid and conclusive histopathological confirmation at one of the two participating institutions between January 2005 and July 2011 were

retrospectively identified from the institutional databases. Thereby, a total of 24 patients [female, 24; mean age, 41.4 ± 11.3 years (range, 20–75 years)] were enrolled. The institutional review boards of both participating institutions approved this study.

Evaluated lesions

In the 24 patients, a total of 34 histopathologically confirmed [liver resection, 28 HCAs in 19 patients; core biopsy (18-gauge biopsy needle; at least 3 samples per lesion), 6 HCAs in 5 patients] HCAs of at least 1 cm in diameter to allow reliable visual and quantitative analysis and without evidence of malignant transformation were present and evaluated. The mean size of the HCAs was 44 ± 33.3 mm (range, 10–141 mm). In ten HCAs, the diameter exceeded 50 mm. Eighteen HCAs were solitary and 16 multiple with a maximum of 4 evaluated HCAs per patient. Two of the 24 patients presented with imaging findings of hepatic adenomatosis (defined as more than 10 visible lesions interpreted as HCAs by similar signal behaviour as the histologically proven lesions).

Magnetic resonance imaging

The MRI data were obtained with 1.5-T systems using phased-array body coils. The examination protocols comprised T2-weighted (w) standard 2D sequences with and without fat saturation (FS) and T1-w unenhanced 2D sequences with and without FS (including in-/opposed phase technique). T1-w 3D sequences with FS (VIBE, WATS, LAVA, or THRIVE) were acquired in breath hold technique before and during the dynamic phase (fixed delay of 20, 50, and 90 s for the arterial, portal venous, and venous phase, respectively) after intravenous application of gadoxetic acid (0.025 mmol/kg body weight; manual or automatic injection at approximately 1–2 ml/s flow rate followed by 40 ml saline flush). In the hepatobiliary plateau phase, T1-w imaging was repeated between 15 and 25 min after contrast administration (3D FS, 2D FS, 2D without FS).

Image analysis

For MRI analysis, a dedicated viewing workstation (Advantage Windows 4.3; GE Healthcare) was used. All cases were read by two independent radiologists (3 and 5 years of experience with gadoxetic acid-enhanced liver MRI) blinded to clinical data in consensus. The following visually assessed parameters were recorded: number of lesions, location, maximum axial diameter, shape (oval, round, or lobulated); margin (ill- or well-defined appearance); presence of fat deposition within the lesion; presence of hemorrhagic and/or necrotic components (i.e. hyperintensities on

unenanced T1-w images with and without FS, cystic components bright on T2-w images, fluid-fluid levels). Lesion intensity was visually compared with the intensity of the surrounding liver parenchyma (hypointense, isointense, hyperintense, mixed).

For quantitative analysis, relative signal intensity (SI) enhancement after contrast administration [(post contrast - precontrast)/precontrast * 100] was calculated from region of interest (ROI) measurements (mean SI values from ROI manually adjusted to cover representative tissue in identical location and size in the different sequences) in the liver (excluding visible vessels and ducts), erector spinae muscle (excluding large interseptations) and HCAs (excluding cystic or hemorrhagic components) for the different contrast phases. A reduction of contrast enhancement of a lesion in the venous phase (so-called “wash out”) was defined quantitatively as a 15 % decrease of SI compared to the highest SI during the preceding enhanced sequences.

As there are no data available from the literature on the relative enhancement of non-hepatocyte-containing liver lesions, a comparison group was created by retrospective identification of patients suffering from histologically proven metastases from non-hepatic adenocarcinomas (breast cancer, 8 patients/15 lesions; colon cancer, 8 patients/9 lesions; female, 11; male, 5; mean age, 61.9 ± 8.8 years; range, 49–76 years) who underwent liver MRI with the same imaging protocol as the patients with HCAs. A maximum of two metastases per patient were evaluated. Exclusion criteria were presence of tumour necrosis, cystic components, or calcification. The relative enhancement of the metastases in the delayed phase was determined according to the method applied to the HCAs.

Statistics

Statistical analyses were performed using the SPSS software (release 11.0.4; SPSS Inc., Chicago, IL) and the R software (version 2.11.1, R Foundation for Statistical Computing, Vienna, Austria). Descriptive parameters are given as mean and standard deviation as well as median and interquartile range (IQR; 25th–75th percentiles). Due to small sample size, normality distribution was not assumed, and in consequence non-parametric tests were performed. Unenhanced and contrast-enhanced uptake in HCA, liver, muscle, and aorta was compared using the non-parametric Wilcoxon test for paired data. Differences between early and late dynamic phase and the hepatobiliary phase were analysed using the non-parametric Friedman test for repeated measurements, and paired tests were performed with the Wilcoxon test with Bonferroni-Holm correction. Differences of relative contrast enhancement of HCA, liver, muscle, and aorta were analysed with the non-parametric Kruskal-Wallis test and the Mann-Whitney U test for unpaired data with Bonferroni-

Holm correction for paired tests. Mann-Whitney U test was used for comparing the relative enhancement of the hepatobiliary phase for HCA versus liver metastasis. All tests were performed two-sided at a 0.05-level for significance.

Results

Morphologic findings

Most HCAs were oval or round (29/34; 85 %); 5 were lobulated (15 %). Most HCAs (91 %) appeared well defined, while 3 HCAs showed ill-defined margins. Three HCAs showed haemorrhage (9 %). Regarding signal intensity, most HCAs were visually hyperintense on T2-w images with (62 %) and without FS (76 %). On unenhanced T1-w images without FS 27 % of lesions were hypointense, 35 % were isointense, 23 % were hyperintense, and 15 % had a mixed appearance. Applying FS, T1-w signal of HCAs was hypointense in 29 %, isointense in 24 %, hyperintense 32 %, and mixed in 15 % of lesions. Fatty content was detected in 44 % (15/34) of HCAs, respectively.

Contrast enhancement

All HCAs showed a mean increase in SI in the arterial phase (74 ± 70 %), the portal venous phase (81 ± 83 %), the venous phase (62 ± 58 %), and the hepatobiliary phase (50 ± 55 %; Tables 1 and 2; Figs. 1 and 2; $P < 0.001$ compared to the unenhanced images). There was no significant difference of the contrast media-related enhancement among the different dynamic phases ($P > 0.05$), even though 13 HCAs (38 %) quantitatively showed reduction of contrast enhancement (“wash out”) in the venous phase compared to the preceding contrast phases. For comparison, SIs of liver, muscle, and aorta are given in Fig. 1.

In the hepatobiliary phase, all HCAs had at least a similar SI as at baseline, while most lesions showed a positive relative enhancement (50 ± 55 %; range, 1–277 %; $P = 0.003$). In a subgroup stratification, the relative enhancement in the hepatobiliary phase was 33 ± 29 % (range, 1–57 %) for the 15 steatotic and 59 ± 65 % (range, 7–277 %) for the 19 non-fatty HCAs ($P < 0.05$). For liver metastases (breast and colon cancer), the SI increase in the hepatobiliary phase was 53 ± 29 % (range, 0–109 %), which was not significantly different from that measured in HCAs ($P = 0.504$; Fig 3). No significant difference was found for the SI increase of the different metastases (breast versus colon cancer) in the hepatobiliary phase, $P > 0.05$.

Comparing HCAs and liver, the relative enhancement of HCAs exceeded that of the liver significantly in the arterial phase ($P < 0.001$), while no significant difference was observed in the portal venous and venous phase ($P = 0.92$ and

Table 1 Change of signal intensity of 34 hepatocellular adenomas and liver during gadoxetic acid-enhanced MRI compared to unenhanced images

Phase	HCAs				Liver			
	Mean	Standard deviation	Minimum	Maximum	Mean	Standard deviation	Minimum	Maximum
Arterial phase	74 %	70 %	1 %	296 %	29 %	28 %	0 %	117 %
Portal venous phase	81 %	83 %	2 %	365 %	76 %	62 %	3 %	246 %
Venous phase	65 %	58 %	0 %	290 %	92 %	77 %	17 %	323 %
Hepatobiliary phase	50 %	55 %	1 %	277 %	116 %	89 %	48 %	376 %

$P=0.35$, respectively); HCA values were significantly lower in the hepatobiliary phase ($P<0.001$).

Upon visual comparison of HCAs to hepatic background on T1-w images with FS in the hepatobiliary phase, 31 out of 34 HCAs (91 %) appeared hypointense. The three remaining lesions were hyperintense ($n=1$) or mixed hypo-/hyperintense ($n=2$). In the subgroup of fatty HCAs, 14 out of 15 (93 %) appeared hypointense and 1 was mixed hyper-/hypointense.

Discussion

The analysis was restricted to histologically proven HCAs. Even though it is known that HCA may occur as multilocular disease, additional lesions in the liver that were not subject to histopathological confirmation were excluded from the analysis regardless of their MRI appearance [21]. Liver adenomatosis, defined as more than ten nodules, is considered a different entity because of the aetiology and prognosis; however, the histological features are basically similar to those of solitary HCAs, which led us to include these cases ($n=2$) [22].

We recorded morphological MRI parameters of all lesions for exact characterisation of our study collective. There are various appearances of HCAs on unenhanced MRI. In comparison with normal liver parenchyma, HCAs have been described as usually hyperintense on T2-w images and mostly hyper- to isointense on T1-w images because of fat and haemorrhagic areas, although some lesions can appear hypointense [7, 20, 23–28]. With the majority of HCAs being hyperintense on T2-w images, a

few large hemorrhagic lesions, and nearly one third of lesions bearing fatty components, the present study cohort can be considered a representative sample in comparison to published series [3, 28, 29].

Histologically, HCAs feature extensive sinusoids and feeding arteries. This explains, that dynamic MRI with extracellular gadolinium chelates often reveals early arterial enhancement [7, 8, 20, 24, 25]. Gadoxetic acid provides intravascular contrast during dynamic perfusion phases and hepatocyte-selective properties during the hepatobiliary phase [11]. Therefore, the typical hyper-enhancement of HCAs in the early dynamic phase with extracellular contrast agents is reproducible using gadoxetic acid as shown in the present study with arterial hyperenhancement in nearly all lesions. On portal venous, venous, and hepatobiliary phases, contrast enhancement is being described to differ depending on the histological type [20, 28]. Lewin et al. stated, that in hepatic adenomatosis full, partial, minimal, or absent enhancement of HCAs can be explained by different types of HCAs [30]. In our study, mean relative enhancement of portal venous and venous phase was rather uniform. However, 13 HCAs presented a “wash-out” of contrast in the venous phase compared to the arterial phase in the quantitative analysis, which is not an uncommon finding in dynamic imaging of HCAs [31]. To differentiate this true “wash-out” from a visual impression of hypointensity because of early onset of hepatocyte-selective uptake in case of gadoxetic acid, quantification in comparison to unenhanced images is necessary.

There has been debate in the past about HCAs being rather hyper- or hypo-enhancing lesions on hepatobiliary

Table 2 Visual enhancement of 34 hepatocellular adenomas during gadoxetic acid-enhanced MRI

Phase	Visual enhancement pattern					
	None	Partial	Complete	Homogeneous	Heterogeneous	Rim
Arterial phase	1	12	20	20	11	2
Portal venous phase	4	12	18	19	7	4
Venous phase	10	9	15	15	8	1
Hepatobiliary phase	31	-	3	1	2	-

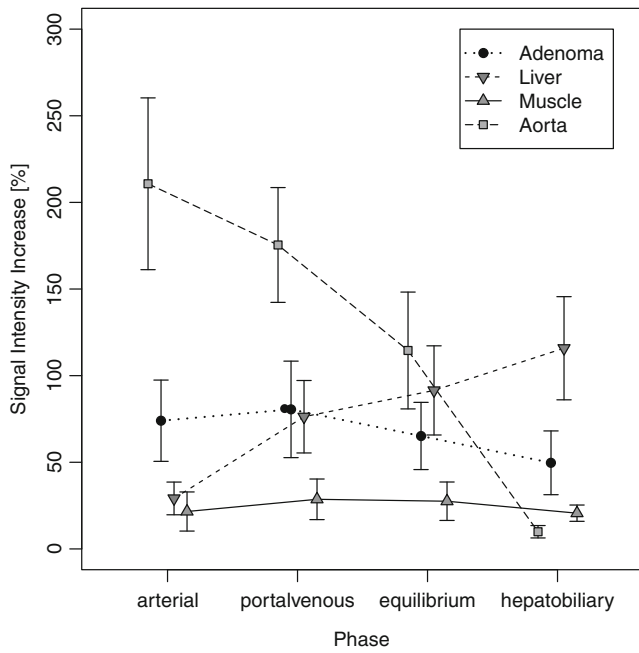


Fig. 1 Mean signal intensity increase with 95 % confidence interval (normalised to unenhanced baseline measurement) of hepatocellular adenomas, liver, and muscle on T1-w fat-saturated images in the different phases of enhancement after application of gadoxetic acid)

phase imaging with a hepatocyte-specific contrast agent. Grazioli et al. found in their study that all HCAs were hypointense on hepatobiliary phase images after application of Gd-BOPTA [25]. For the use of gadoxetic acid, HCAs are

Fig. 2 A 42-year-old female patient with hepatocellular adenoma examined with gadoxetic acid-enhanced MRI (a pre-contrast T1-w fat saturated; b T2-w; T1-w fat saturated images of the c arterial, d portal venous, e venous phase, and f hepatobiliary phase)

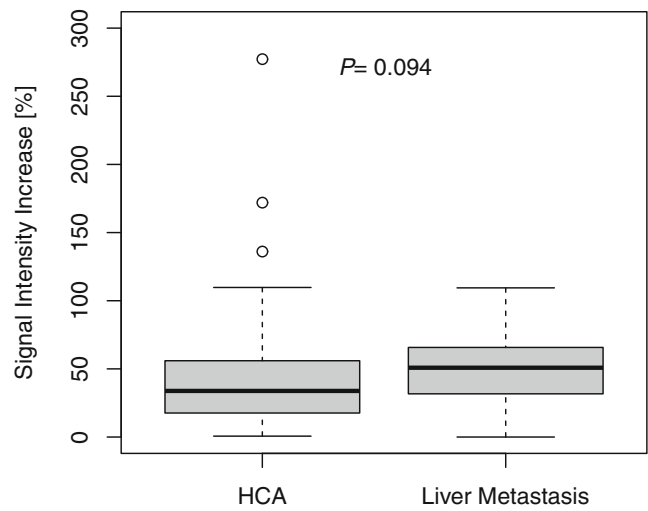
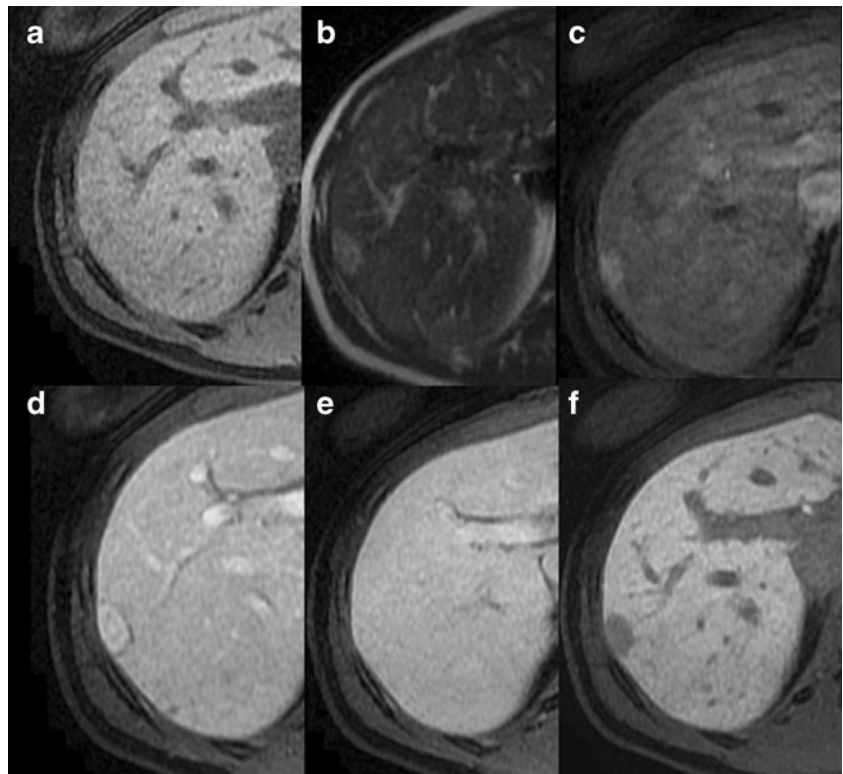


Fig. 3 Signal intensity increase of hepatocellular adenomas and liver metastases after application of gadoxetic acid in the hepatobiliary phase

believed to typically appear hypointense on hepatobiliary phase images as well because of the lack of biliary canaliculi; this, however, lacks data and therefore cannot be considered as proven [25]. Contradictorily, some HCAs are reported to appear iso- or even hyperintense to the liver on hepatobiliary phase imaging, while the underlying uptake mechanism has not been investigated [12]. No larger series are currently available looking specifically at MRI of HCAs with gadoxetic acid. There are so far three reports with small case numbers in the literature dealing with the MRI

appearance of HCAs using gadoxetic acid [10, 11, 20]. In one study with three cases of adenomatosis, only a minority of lesions showed strong, diffuse, or peripheral visual enhancement in the hepatobiliary phase [20]. In a study of Huppertz et al., two out of three HCAs showed visual enhancement compared to the surrounding liver tissue on hepatobiliary phase images [11]. In the present study, uniformly all HCAs showed a significant contrast uptake in the hepatobiliary phase upon quantitative analysis, which was, however, significantly lower compared with the surrounding liver parenchyma. Interestingly, the contrast uptake of HCAs in the present analysis was not higher than that of non-hepatocyte-derived lesions (metastases from breast and colon cancer) in the control group. This can be explained by non-specific pooling in the tumour's interstitium (possibly applying to HCAs and metastases alike) and accumulation in fibrotic partitions. Whether there is some specific cellular uptake of gadoxetic acid in HCAs remains unclear but it is questionable whether measurement of relative Gd-EOB enhancement of HCAs during the hepatobiliary phase could serve as a discriminator from metastatic disease. A limitation of the study regarding this conclusion is the quantification method used. For SI measurement we did not use phantoms to correct for signal-to-noise ratios and had to use normalisation with unenhanced baseline images because varying MR devices and sequences had been employed.

Visually, three HCAs were at least partially hyperintense to the surrounding liver parenchyma on T1-w hepatobiliary phase images with FS. It can be debated whether these HCAs could represent a certain histological HCA subtype. However, HCAs with fatty content, which is believed to be an important discriminator of a certain subgroup of HCAs [28, 32–36], showed both hypointensity (93 % of lesions) and hyperintensity (7 % of lesions) in a similar proportion as the non-steatotic HCAs (90 and 10 %, respectively). So far, histopathological reassessment of the adenomas regarding the sub-classification recently proposed by Bioulac-Sage et al. [33], which was not routine at our institutions in the past, is not available for all cases because of an insufficient amount of archived tissue samples or pending analysis. Therefore, conclusions cannot be drawn on this issue. Further studies and larger case numbers are needed to clarify a possible correlation of histological type, OATP expression, and late gadoxetic acid enhancement.

In summary, the typical contrast behaviour of HCAs during the early dynamic vascular phases known from extracellular CT and MRI contrast media is reproducible when gadoxetic acid-enhanced MRI is used. During the hepatobiliary phase of gadoxetic acid, contrast accumulation in HCAs can be present, although in the vast majority significantly less than in the liver. Thus, the typical HCA appearance is a hypointense lesion in hepatobiliary phase images. True hyperintense HCAs during the hepatobiliary phase may rarely occur.

References

1. Soe KL, Soe M, Gluud C (1992) Liver pathology associated with the use of anabolic-androgenic steroids. *Liver* 12:73–9
2. van den Esschert JW, van Gulik TM, Phoa SS (2010) Imaging modalities for focal nodular hyperplasia and hepatocellular adenoma. *Dig Surg* 27:46–55
3. van der Windt DJ, Kok NF, Hussain SM, Zondervan PE, Alwayn IP, de Man RA et al (2006) Case-orientated approach to the management of hepatocellular adenoma. *Br J Surg* 93:1495–502
4. Shanbhogue AK, Prasad SR, Takahashi N, Vikram R, Sahani DV (2011) Recent advances in cytogenetics and molecular biology of adult hepatocellular tumors: implications for imaging and management. *Radiology* 258:673–93
5. Barthelmes L, Tait IS (2005) Liver cell adenoma and liver cell adenomatosis. *HPB (Oxford)* 7:186–96
6. Stoot JH, Coelen RJ, De Jong MC, Dejong CH (2010) Malignant transformation of hepatocellular adenomas into hepatocellular carcinomas: a systematic review including more than 1600 adenoma cases. *HPB (Oxford)* 12:509–22
7. Ba-Salamah A, Uffmann M, Saini S, Bastati N, Herold C, Schima W (2009) Clinical value of MRI liver-specific contrast agents: a tailored examination for a confident non-invasive diagnosis of focal liver lesions. *Eur Radiol* 19:342–57
8. Morana G, Grazioli L, Kirchin MA, Bondioni MP, Faccioli N, Guarise A et al (2011) Solid hypervascular liver lesions: accurate identification of true benign lesions on enhanced dynamic and hepatobiliary phase magnetic resonance imaging after gadobenate dimeglumine administration. *Invest Radiol* 46:225–39
9. Bluemke DA, Sahani D, Amendola M, Balzer T, Breuer J, Brown JJ et al (2005) Efficacy and safety of MR imaging with liver-specific contrast agent: US multicenter phase III study. *Radiology* 237:89–98
10. Halavaara J, Breuer J, Ayuso C, Balzer T, Bellin MF, Blomqvist L et al (2006) Liver tumor characterization: comparison between liver-specific gadoxetic acid disodium-enhanced MRI and biphasic CT—a multicenter trial. *J Comput Assist Tomogr* 30:345–54
11. Huppertz A, Haraida S, Kraus A, Zech CJ, Scheidler J, Breuer J et al (2005) Enhancement of focal liver lesions at gadoxetic acid-enhanced MR imaging: correlation with histopathologic findings and spiral CT—initial observations. *Radiology* 234:468–78
12. Ringe KI, Husarik DB, Sirlin CB, Merkle EM (2010) Gadoxetate disodium-enhanced MRI of the liver: part 1, protocol optimization and lesion appearance in the noncirrhotic liver. *AJR Am J Roentgenol* 195:13–28
13. Huppertz A, Breuer J, Fels LM, Schultze-Mosgau M, Sutter G, Klein S et al (2011) Evaluation of possible drug-drug interaction between gadoxetic acid and erythromycin as an inhibitor of organic anion transporting peptides (OATP). *J Magn Reson Imaging* 33:409–16
14. Leonhardt M, Keiser M, Oswald S, Kuhn J, Jia J, Grube M et al (2010) Hepatic uptake of the magnetic resonance imaging contrast agent Gd-EOB-DTPA: role of human organic anion transporters. *Drug Metab Dispos* 38:1024–8
15. Narita M, Hatano E, Arizono S, Miyagawa-Hayashino A, Isoda H, Kitamura K et al (2009) Expression of OATP1B3 determines uptake of Gd-EOB-DTPA in hepatocellular carcinoma. *J Gastroenterol* 44:793–8
16. van Montfoort JE, Stieger B, Meijer DK, Weinmann HJ, Meier PJ, Fattinger KE (1999) Hepatic uptake of the magnetic resonance imaging contrast agent gadoxetate by the organic anion transporting polypeptide Oatp1. *J Pharmacol Exp Ther* 290:153–7
17. Hamm B, Staks T, Muhler A, Bollow M, Taupitz M, Frenzel T et al (1995) Phase I clinical evaluation of Gd-EOB-DTPA as a

- hepatobiliary MR contrast agent: safety, pharmacokinetics, and MR imaging. *Radiology* 195:785–92
18. Kato N, Yokawa T, Tamura A, Heshiki A, Ebert W, Weinmann HJ (2002) Gadolinium-ethoxybenzyl-diethylenetriamine-pentaacetic acid interaction with clinical drugs in rats. *Invest Radiol* 37:680–4
 19. Tsuboyama T, Onishi H, Kim T, Akita H, Hori M, Tatsumi M et al (2010) Hepatocellular carcinoma: hepatocyte-selective enhancement at gadoxetic acid-enhanced MR imaging—correlation with expression of sinusoidal and canalicular transporters and bile accumulation. *Radiology* 255:824–33
 20. Giovanoli O, Heim M, Terracciano L, Bongartz G, Ledermann HP (2008) MRI of hepatic adenomatosis: initial observations with gadoxetic acid contrast agent in three patients. *AJR Am J Roentgenol* 190:W290–3
 21. Rebouissou S, Bioulac-Sage P, Zucman-Rossi J (2008) Molecular pathogenesis of focal nodular hyperplasia and hepatocellular adenoma. *J Hepatol* 48:163–70
 22. Flejou JF, Barge J, Menu Y, Degott C, Bismuth H, Potet F et al (1985) Liver adenomatosis. An entity distinct from liver adenoma? *Gastroenterology* 89:1132–8
 23. Arrive L, Flejou JF, Vilgrain V, Belghiti J, Najmark D, Zins M et al (1994) Hepatic adenoma: MR findings in 51 pathologically proved lesions. *Radiology* 193:507–12
 24. Chung KY, Mayo-Smith WW, Saini S, Rahmouni A, Golli M, Mathieu D (1995) Hepatocellular adenoma: MR imaging features with pathologic correlation. *AJR Am J Roentgenol* 165:303–8
 25. Grazioli L, Morana G, Kirchin MA, Schneider G (2005) Accurate differentiation of focal nodular hyperplasia from hepatic adenoma at gadobenate dimeglumine-enhanced MR imaging: prospective study. *Radiology* 236:166–77
 26. Hussain SM, van den Bos IC, Dwarkasing RS, Kuiper JW, den Hollander J (2006) Hepatocellular adenoma: findings at state-of-the-art magnetic resonance imaging, ultrasound, computed tomography and pathologic analysis. *Eur Radiol* 16:1873–86
 27. Paulson EK, McClellan JS, Washington K, Spritzer CE, Meyers WC, Baker ME (1994) Hepatic adenoma: MR characteristics and correlation with pathologic findings. *AJR Am J Roentgenol* 163:113–6
 28. van Aalten SM, Thomeer MG, Terkivatan T, Dwarkasing RS, Verheij J, de Man RA et al (2011) Hepatocellular adenomas: correlation of MR imaging findings with pathologic subtype classification. *Radiology* 261:172–81
 29. Vetelainen R, Erdogan D, de Graaf W, ten Kate F, Jansen PL, Gouma DJ et al (2008) Liver adenomatosis: re-evaluation of aetiology and management. *Liver Int* 28:499–508
 30. Lewin M, Handra-Luca A, Arrive L, Wendum D, Paradis V, Bridel E et al (2006) Liver adenomatosis: classification of MR imaging features and comparison with pathologic findings. *Radiology* 241:433–40
 31. Ricci P, Cantisani V, D'Onofrio M, Sahani D, Pagliara E, Calliada F et al (2008) Behavior of hepatocellular adenoma on real-time low-mechanical index contrast-enhanced ultrasonography with a second-generation contrast agent. *J Ultrasound Med* 27:1719–26
 32. Bioulac-Sage P, Balabaud C, Zucman-Rossi J (2010) Focal nodular hyperplasia, hepatocellular adenomas: past, present, future. *Gastroenterol Clin Biol* 34:355–8
 33. Bioulac-Sage P, Balabaud C, Zucman-Rossi J (2010) Subtype classification of hepatocellular adenoma. *Dig Surg* 27:39–45
 34. Bioulac-Sage P, Blanc JF, Rebouissou S, Balabaud C, Zucman-Rossi J (2007) Genotype phenotype classification of hepatocellular adenoma. *World J Gastroenterol* 13:2649–54
 35. Bioulac-Sage P, Laumonier H, Couchy G, Le Bail B, Sa Cunha A, Rullier A et al (2009) Hepatocellular adenoma management and phenotypic classification: the Bordeaux experience. *Hepatology* 50:481–9
 36. Bioulac-Sage P, Rebouissou S, Thomas C, Blanc JF, Saric J, Sa Cunha A et al (2007) Hepatocellular adenoma subtype classification using molecular markers and immunohistochemistry. *Hepatology* 46:740–8